

1T phase as an efficient hole injection layer to TMDs transistors: a universal approach to achieve p-type contacts

Hu, X.; Wang, Y.; Shen, X.; Krasheninnikov, A. V.; Sun, L.; Chen, Z.;

Originally published:

June 2018

2D Materials 5(2018), 031012

DOI: <https://doi.org/10.1088/2053-1583/aac859>

Perma-Link to Publication Repository of HZDR:

<https://www.hzdr.de/publications/Publ-27823>

Release of the secondary publication
on the basis of the German Copyright Law § 38 Section 4.

ACCEPTED MANUSCRIPT

1T phase as an efficient hole injection layer to TMDs transistors: A universal approach to achieve p-type contacts

To cite this article before publication: Xiaohui Hu *et al* 2018 *2D Mater.* in press <https://doi.org/10.1088/2053-1583/aac859>

Manuscript version: Accepted Manuscript

Accepted Manuscript is “the version of the article accepted for publication including all changes made as a result of the peer review process, and which may also include the addition to the article by IOP Publishing of a header, an article ID, a cover sheet and/or an ‘Accepted Manuscript’ watermark, but excluding any other editing, typesetting or other changes made by IOP Publishing and/or its licensors”

This Accepted Manuscript is © 2018 IOP Publishing Ltd.

During the embargo period (the 12 month period from the publication of the Version of Record of this article), the Accepted Manuscript is fully protected by copyright and cannot be reused or reposted elsewhere.

As the Version of Record of this article is going to be / has been published on a subscription basis, this Accepted Manuscript is available for reuse under a CC BY-NC-ND 3.0 licence after the 12 month embargo period.

After the embargo period, everyone is permitted to use copy and redistribute this article for non-commercial purposes only, provided that they adhere to all the terms of the licence <https://creativecommons.org/licenses/by-nc-nd/3.0>

Although reasonable endeavours have been taken to obtain all necessary permissions from third parties to include their copyrighted content within this article, their full citation and copyright line may not be present in this Accepted Manuscript version. Before using any content from this article, please refer to the Version of Record on IOPscience once published for full citation and copyright details, as permissions will likely be required. All third party content is fully copyright protected, unless specifically stated otherwise in the figure caption in the Version of Record.

View the [article online](#) for updates and enhancements.

**1T Phase as an Efficient Hole Injection Layer to TMDs Transistors:
A Universal Approach to Achieve p-type Contacts**

Xiaohui Hu,^{*1,2} Yifeng Wang,^{1,2} Xiaodong Shen,^{1,2} Arkady V. Krasheninnikov,^{3,4}

Litao Sun,^{*5} Zhongfang Chen^{*6}

¹ College of Materials Science and Engineering, Nanjing Tech University, Nanjing 210009, China

² Jiangsu Collaborative Innovation Center for Advanced Inorganic Function Composites, Nanjing Tech University, Nanjing 210009, China

³ Institute of Ion Beam Physics and Materials Research, Helmholtz-Zentrum Dresden-Rossendorf, 01314 Dresden, Germany

⁴ Department of Applied Physics, Aalto University School of Science, PO Box 11100, 00076 Aalto, Finland

⁵ SEU-FEI Nano-Pico Center, Key Laboratory of MEMS of Ministry of Education, Collaborative Innovation Center for Micro/Nano Fabrication, Device and System, Southeast University, Nanjing 210096, China

⁶ Department of Chemistry, University of Puerto Rico, Rio Piedras Campus, San Juan, Puerto Rico 00931

Corresponding Author:

xiaohui.hu@njtech.edu.cn (XH); slt@seu.edu.cn (LS); zhongfangchen@gmail.com (ZC)

Abstract

Recently, the fabricated MoS₂ field effect transistors (FETs) with 1T-MoS₂ electrodes exhibit excellent performance with rather low contact resistance, as compared with those with metals deposited directly on 2H-MoS₂ [*Nat. Mater.* **2014**, *13*, 1128], but the reason for that remains elusive. By means of density functional theory calculations, we investigated the carrier injection at the 1T/2H MoS₂ interface and found that although the Schottky barrier height (SBH) values of 1T/2H MoS₂ interfaces can be tuned by controlling the stacking patterns, the p-type SBH values of 1T/2H MoS₂ interfaces with different stackings are lower than their corresponding n-type SBH values, which demonstrated that the metallic 1T phase can be used as an efficient hole injection layer for 2H-MoS₂. In addition, as compared to the n-type Au/MoS₂ and Pd/MoS₂ contacts, the p-type SBH values of 1T/2H MoS₂ interfaces are much lower, which stem from the efficient hole injection between 1T-MoS₂ and 2H-MoS₂. This can explain the low contact resistance in the MoS₂ FETs with 1T-MoS₂ electrodes. Notably, the SBH values can be effectively modulated by an external electric field, and a significantly low p-type SBH value can be achieved under an appropriate electric field. We also demonstrated that this approach is also valid for WS₂, WSe₂ and MoSe₂ systems, which indicates that the method can most likely be extended to other TMDs, and thus may open new promising avenues of contact engineering in these materials.

Introduction

Two-dimensional (2D) transition metal dichalcogenides (TMDs) have recently received great attention as the channel material for FETs [1–8]. In principle, TMD FETs can transport either electrons (n-FET) or holes (p-FET) in the conducting channel, depending on the height of the Schottky barrier relative to the conduction band minimum (CBM) or valence-band maximum (VBM) [9]. However, most experimentally reported TMD FETs based on a Schottky device architecture are of n-type probably due to the relative ease of fabrication [9–12]. To complement TMDs for digital logic applications, it is highly desirable to develop p-type TMD-based FETs [13]. However, the studies of p-type TMD FETs are rather scarce due to the fabrication difficulties [9]. Thus, significant efforts have been undertaken to achieve efficient hole contacts. Experimentally, p-type multilayer MoS₂ FETs have been manufactured through hole-doping by palladium (Pd) contacts in the limit of large gate fields [14]. Recently, molybdenum trioxide (MoO_x, $x < 3$) [9, 15], a high work function material, was used as a buffer layer between Pd and MoS₂/WSe₂, and showed an efficient hole injection to MoS₂ and WSe₂. In particular, FETs made from single-layer MoS₂, a semiconductor with a direct band gap of 1.8 eV [1, 16], high carrier mobility ($\sim 200 \text{ cm}^2/\text{Vs}$) and excellent on/off current ratio (10^8) [17], demonstrate appealing performance. According to recent density functional theory (DFT) calculations [18–20], various metals can contact with MoS₂ to form n-type transistors, since the Fermi level of elemental metals is pinned close to the CBM of MoS₂. In stark contrast, among numerous metals examined (including Al, Ag, Au, Pd,

Ir, Pt, Ru, Ni, Sc and Ti), only in the case of platinum, a p-type Schottky contact was computationally identified at the Pt/MoS₂ interface [18, 20]. In addition, graphene oxide (GO) was proposed to be a promising hole injection layer for single-layer MoS₂ due to its high work function and the relatively weak Fermi level pinning at the interfaces, and the p-type SBH can be decreased significantly by increasing the oxygen concentration as well as the fraction of epoxy functional groups in GO [21]. However, GO is nonstoichiometric, and it is rather challenging to experimentally control the oxygen concentration and the epoxy to hydroxyl ratio [22].

Monolayer TMDs have three polymorphs, namely trigonal prismatic (2H), octahedral (1T), and distorted 1T(1T') [23], among which the semiconducting 2H phase is energetically most favorable and has the highest stability. The phase transformations from the 2H-MoS₂ to the metallic 1T-MoS₂ can be induced by electron beam [24, 25] or lithium or sodium ion intercalation [26, 27]. Note that 1T-MoS₂ can exist even after complete removal of the ion support, although this phase is stabilized by electron donation via ion intercalation during synthesis [28, 29]. Recent experiments clearly demonstrated the advantages of 1T-MoS₂ over 2H-MoS₂ for some applications: 1T-MoS₂ shows higher catalytic activity for hydrogen evolution reactions (HER) [30, 31]. Especially, Kappera *et al.* found that, as compared with those with metals deposited directly on 2H-MoS₂, FETs with locally introduced 1T-MoS₂ (with ~70% concentration) electrodes exhibited superior performance with rather low contact resistance, and expected that the FETs with pure 1T phase could have even greater enhancement in performance [27, 32]. Then, a

question raises naturally, why do MoS₂ FETs with 1T phase electrodes exhibit excellent performance? How does the carrier injection occur at the 1T/2H MoS₂ interface? Can such an approach be extended to other TMDs?

In this work, by means of systematic DFT calculations, we studied the carrier injection at the 1T/2H MoS₂ interface and demonstrated that the metallic 1T phase can be used as an efficient hole injection layer for 2H-MoS₂. We show that 1T-MoS₂ forms a p-type contact with 2H-MoS₂, and the p-type SBH values are lower than those of the n-type Au/MoS₂ and Pd/MoS₂ contacts [18], which stem from the efficient hole injection between 1T-MoS₂ and 2H-MoS₂. This can explain the low contact resistance in the MoS₂ FETs with 1T-MoS₂ electrodes [27]. Notably, we find that an external electric field is able to effectively modulate the band alignment of 1T/2H MoS₂ interfaces, and the SBH values can be reduced or enhanced depending on the magnitude and direction of the electric field, and a significantly low p-type SBH value can be achieved under an appropriate electric field. Finally, we extend our studies to other TMDs, such as WS₂, WSe₂ and MoSe₂, and find that the p-type contacts are also obtained in their 1T/2H interfaces.

Computational Method

Our DFT calculations were performed using the VASP package [33, 34]. The projector-augmented-wave (PAW) method was employed to describe electron-ion interactions [35, 36], while the exchange-correlation functional was treated by generalized gradient approximation (GGA) in the scheme of Perdew-Burke-Ernzerhof (PBE) [37]. Van der Waals corrections were included through Grimme's DFT-D2

method as implemented in VASP [38, 39]. The energy cutoff of the plane wave was set to 500 eV, and the atomic positions were fully relaxed until the maximum force on each atom was less than 0.005 eV/Å. A k-point sampling of $32 \times 32 \times 1$ was used for geometry optimizations and self-consistent calculations, and a vacuum region of 16 Å was introduced to avoid interaction between periodic images of slabs. Note that in DFT calculations, 1T phase can spontaneously transform into the 1T'-MoS₂ [40], but the difference between these two phases is rather small. Moreover, 1T phase was experimentally synthesized [27, 32]. Thus, in this work we adapted the 1T-MoS₂ phase instead of 1T'-MoS₂, as it gives the qualitatively correct picture and the computed SBH trends are not affected (see figures S1, S2 and the related text in Supporting Information). In addition, the spin-orbit interactions were not accounted here, as it does not affect the p-type SBH trends (see figure S3 in the Supporting Information for details).

Results and discussion

In order to construct the 1T/2H MoS₂ interfaces, we first examined the lattice constants of 1T-MoS₂ and 2H-MoS₂ monolayers. The calculated lattice constants of 1T and 2H phases of MoS₂ are the same (3.18 Å), well consistent with previous results [41]. Thus, the 1T/2H MoS₂ interfaces can be constructed simply by stacking the primitive cells of 1T-MoS₂ and 2H-MoS₂ without any strain. Note that there are three high-symmetry sites in monolayer 2H-MoS₂: S-site (denoted as A), Mo-site (B), and center-of-hexagon (C). All the 1T/2H MoS₂ interfaces can be built using these sites.

For example, as shown in figure 1(a), monolayer 2H-MoS₂ can be named as ABA,

while monolayer 1T-MoS₂ is denoted as ABC according to the atomic stacking sequence (S'-Mo-S). For all the 1T/2H MoS₂ interfaces in this work, the bottom layer is always 2H-MoS₂ (ABA), while the top 1T-MoS₂ layer has totally six different atomic sequences when stacked above 2H-MoS₂, namely ABC, ACB, BAC, BCA, CAB and CBA (figure 1(a)-(f)). Because one layer is always 2H-MoS₂ (ABA), for simplicity, we used the atomic stacking sequence of 1T-MoS₂ to name these six different stackings of 1T/2H MoS₂ (figure 1).

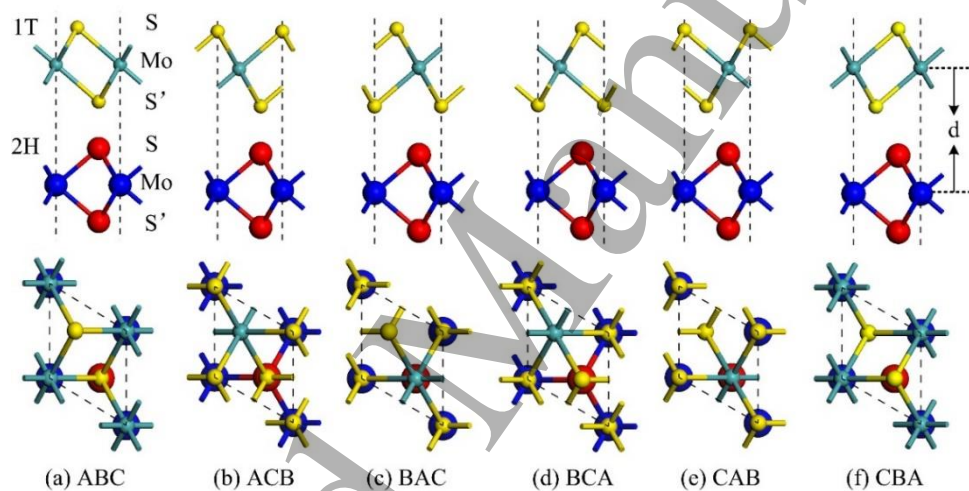


Figure 1. The top and side views of six different stackings of 1T and 2H MoS₂ sheets.

The definition for the interlayer distance d is indicated in panel (f).

To investigate the stability of the 1T/2H MoS₂ interfaces, we computed the interlayer binding energy, which is defined as the energy difference between 1T/2H MoS₂ and the corresponding monolayers ($E_b = E_{1T/2H} - E_{1T} - E_{2H}$) (see the related text in Supporting Information). According to this definition, a more negative E_b value indicates a higher stability of the interface. As summarized in Table 1, the interlayer

binding energies of ABC and ACB stacked 1T/2H MoS₂ (-0.10 eV) are slightly less negative than those of BAC, BCA, CAB and CBA stacked 1T/2H MoS₂ (-0.15~-0.17 eV), which indicates that the ABC and ACB stacked 1T/2H MoS₂ are less favorable than the others. Overall, all the interlayer binding energies are negative, suggesting that all these 1T/2H MoS₂ interfaces are energetically favorable.

The interfacial distances well correlate with the interlayer binding energies for 1T/2H MoS₂ interfaces. Specifically, the interfacial distance d is significantly larger in the energetically less favorable ABC and ACB stacked 1T/2H MoS₂ (6.83 and 6.75 Å, respectively) than other stackings (6.14~6.24Å). Note that the equilibrium distance between monolayer 2H-MoS₂ and 1T-MoS₂ depends on the relative position of S atoms at the interface. When S atoms at the interface are stacked directly on top of each other, the interlayer coupling between the two monolayers is weaker, leading to the increased interlayer distance and less favorable binding energy for ABC and ACB stacked 1T/2H MoS₂. In contrast, when S atoms at the interface are staggered, the interlayer coupling becomes stronger, leading to a decreased interlayer distance and stronger binding energy in BAC, BCA, CAB and CBA stacked 1T/2H MoS₂ (Table1).

Table 1. The interlayer binding energy E_b (eV/f.u.), the equilibrium interfacial distance d (Å) between the 1T-MoS₂ Mo plane and the 2H-MoS₂ Mo plane, the n-type SBH values (n-SBH), and the p-type SBH values (p-SBH) in the 1T/2H MoS₂ interfaces.

	E_b (eV/f.u.)	d (Å)	n-SBH (eV)	p-SBH (eV)
ABC	-0.10	6.83	0.81	0.67
ACB	-0.10	6.75	0.83	0.65
BAC	-0.17	6.24	0.79	0.49
BCA	-0.16	6.14	0.70	0.48
CAB	-0.16	6.19	0.82	0.44
CBA	-0.15	6.23	0.75	0.49

The electronic properties of 2H-MoS₂ and 1T-MoS₂ are quite different. At the PBE level of theory, 2H-MoS₂ is semiconducting with a direct band gap of 1.68 eV, while 1T-MoS₂ is metallic (figure S4, Supporting Information). Our results agree well with previous theoretical calculations [41]. SBH is a key factor that determines contact resistances in the MoS₂ transistors [42]. According to previous DFT simulations on GO/MoS₂ interfaces [21] and metal/MoS₂ contacts [18], the n-type SBH is defined as the energy difference between the Fermi level of the interfaces and the CBM of 2H-MoS₂ layer, while the p-type SBH is the energy difference between the VBM of 2H-MoS₂ layer and the Fermi level of the interfaces. Therefore, we computed the band structures (figure 2(a)-(f)), the total density of states (TDOS) of the 1T/2H MoS₂

1
2
3
4 interfaces and the projected density of states (PDOS) from 2H-MoS₂, 1T-MoS₂ of the
5
6
7 interfaces (figure S5, Supporting Information), then obtained the SBH values by
8
9
10 comparing the band structures and DOS of the interfaces with those of 2H-MoS₂ from
11
12 the interfaces. To gain further insight, we carefully checked the band alignment for
13
14 monolayer 2H-MoS₂, monolayer 1T-MoS₂ and 1T/2H MoS₂ interfaces (figure 2(g)),
15
16
17 and found that the work function ($W = E_{\text{vac}} - E_{\text{F}}$, where E_{vac} and E_{F} are the vacuum
18
19 level and Fermi level, respectively) of 1T-MoS₂ is closer to the VBM than to the CBM
20
21 of 2H-MoS₂, indicating that 1T-MoS₂ can be used as a hole contact for 2H-MoS₂.
22
23
24 Meanwhile, the Fermi level slightly shifts up after 2H-MoS₂ and 1T-MoS₂ form the
25
26
27 1T/2H MoS₂ interfaces. Thus, the work function of the 1T/2H MoS₂ interfaces is
28
29
30 slightly smaller than that of monolayer 2H-MoS₂ and monolayer 1T-MoS₂ (figure
31
32
33 2(g)).
34
35
36
37
38
39
40
41
42
43
44
45
46
47
48
49
50
51
52
53
54
55
56
57
58
59
60

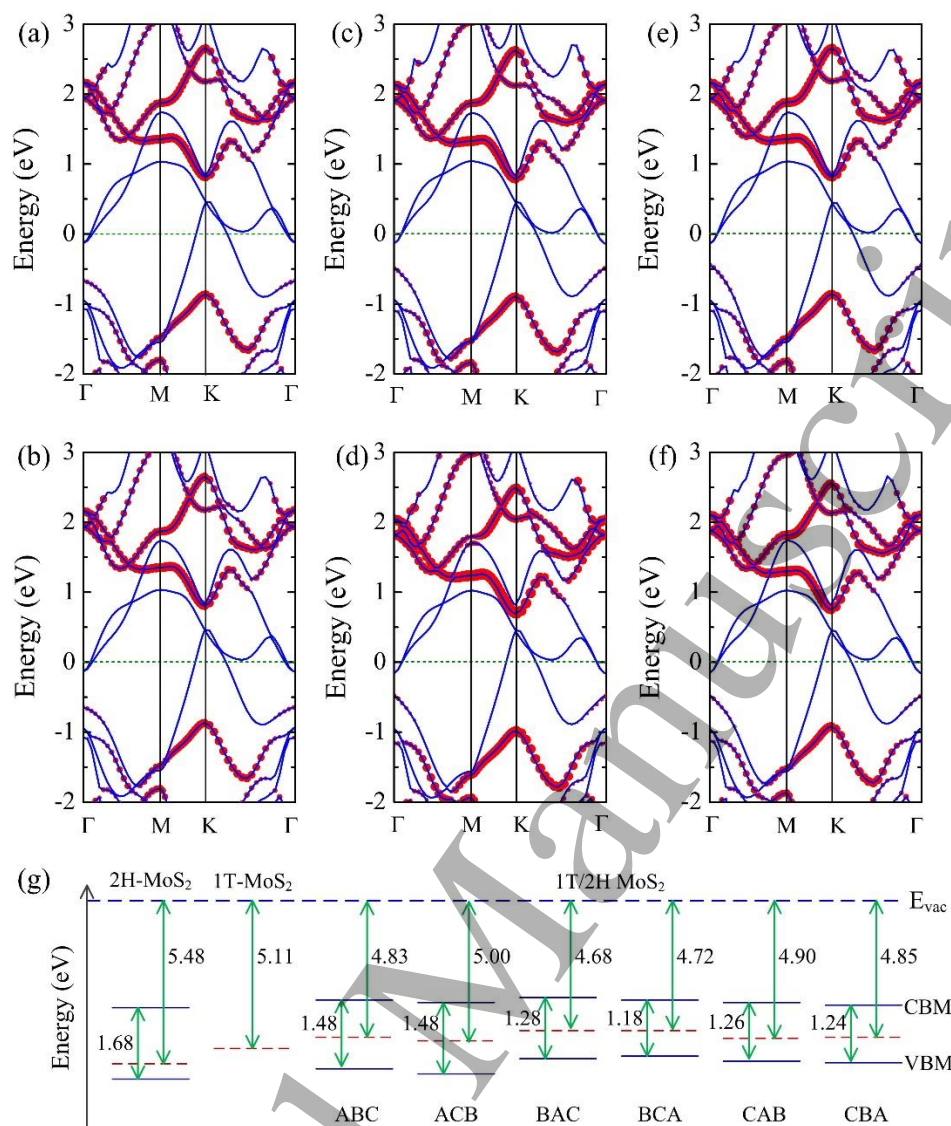


Figure 2. Band structures of 1T/2H MoS₂ interfaces with different stackings of (a) ABC, (b) ACB, (c) BAC, (d) BCA, (e) CAB, and (f) CBA, respectively. The blue solid lines are the overall band structures. The red dots denote the projected band structures of the 2H-MoS₂ layer. The weight is represented by the dot size. The Fermi level is set at zero, indicated by the olive dashed lines. (g) Band alignments of monolayer 2H-MoS₂, monolayer 1T-MoS₂ and 1T/2H MoS₂ interfaces. Relevant electronic parameters are also given. The red dashed lines are the Fermi level. The vacuum level is taken as reference.

Table 1 summarizes the computed n-type and p-type SBH values of the 1T/2H MoS₂ interfaces with different stacking configurations. Notably, the maximal difference in the n-type SBH is 0.13 eV, while that in the p-type SBH is 0.23 eV. Thus, there is a partial Fermi level pinning behavior at the interface, in other words, the Fermi levels are in a 0.13-0.23 eV window in the gap for these six interfacial configurations. Our computations also suggest that the SBH values at the 1T/2H MoS₂ interfaces can be tuned by controlling the stacking patterns.

Interestingly, distinct from most metal/MoS₂ contacts [18], the Fermi level is closer to the VBM than to the CBM of 2H-MoS₂ (figure 2), indicating that all these 1T/2H MoS₂ interfaces form p-type contacts. Furthermore, the p-type SBH values (0.44–0.67 eV) are lower than those of the n-type Au/MoS₂ and Pd/MoS₂ contacts (0.88 and 0.85 eV, respectively) [18], which result from the efficient hole injection between 1T-MoS₂ and 2H-MoS₂. This can explain the low contact resistance in the MoS₂ FETs with 1T phase electrodes [27]. Note that Au and Pd are the most common electrode materials, and were also used in Kappera's studies on the MoS₂ FETs with 1T-MoS₂ electrodes [27]. In order to compare the performance of MoS₂ FETs with pure 1T electrodes and locally introduced 1T-MoS₂ electrodes, taking the BAC stacked 1T/2H MoS₂ interfaces as an example, we calculated the total DOS, the PDOS of 2H-MoS₂ and locally introduced 1T-MoS₂ (figures S6 and S7). It is found that the p-type SBH value (0.49 eV) of 1T/2H MoS₂ with pure 1T-MoS₂ is lower than those of 1T/2H MoS₂ with locally introduced 1T-MoS₂ (0.57 eV). Our above analysis strongly supports Kappera *et al*'s expectation that MoS₂ FETs with pure 1T phase electrodes will have even

greater enhancement in performance than those with locally introduced 1T-MoS₂ electrodes [27].

The pristine 2H-MoS₂ monolayer exhibits a direct band gap at the K point (figure S4), its CBM is mostly contributed by Mo d_z^2 orbitals, while its VBM is composed of mainly Mo d_{xy} and $d_{x^2-y^2}$ orbitals. With increasing the number of layers, the VB edge at Γ point dominated by Mo d_z^2 orbitals becomes important and increases rapidly [43]. The similar trend occurs when 1T-MoS₂ is added to 2H-MoS₂ to form 1T/2H MoS₂ interfaces: the VBM of 2H-MoS₂ in all the 1T/2H MoS₂ interfaces is dominated by Mo d_z^2 orbitals, instead of Mo d_{xy} and $d_{x^2-y^2}$ orbitals as in the pristine 2H-MoS₂ monolayer (figure 3), and is shifted from K point to Γ point (figure 2). On the other hand, as compared with the pristine 2H-MoS₂ monolayer, in 1T/2H MoS₂ interfaces the conduction bands of 2H-MoS₂ are well preserved with the CBM located at the K point (figure 2). Clearly, upon the formation of the 1T/2H MoS₂ interfaces, the VB edge at Γ point of the pristine 2H-MoS₂ shifts to the VBM in 1T/2H MoS₂ interfaces, which explains the decrease of the band gap of 2H-MoS₂ (figure 2(g)) and the achievement of the p-type SBH in the 1T/2H MoS₂ interfaces.

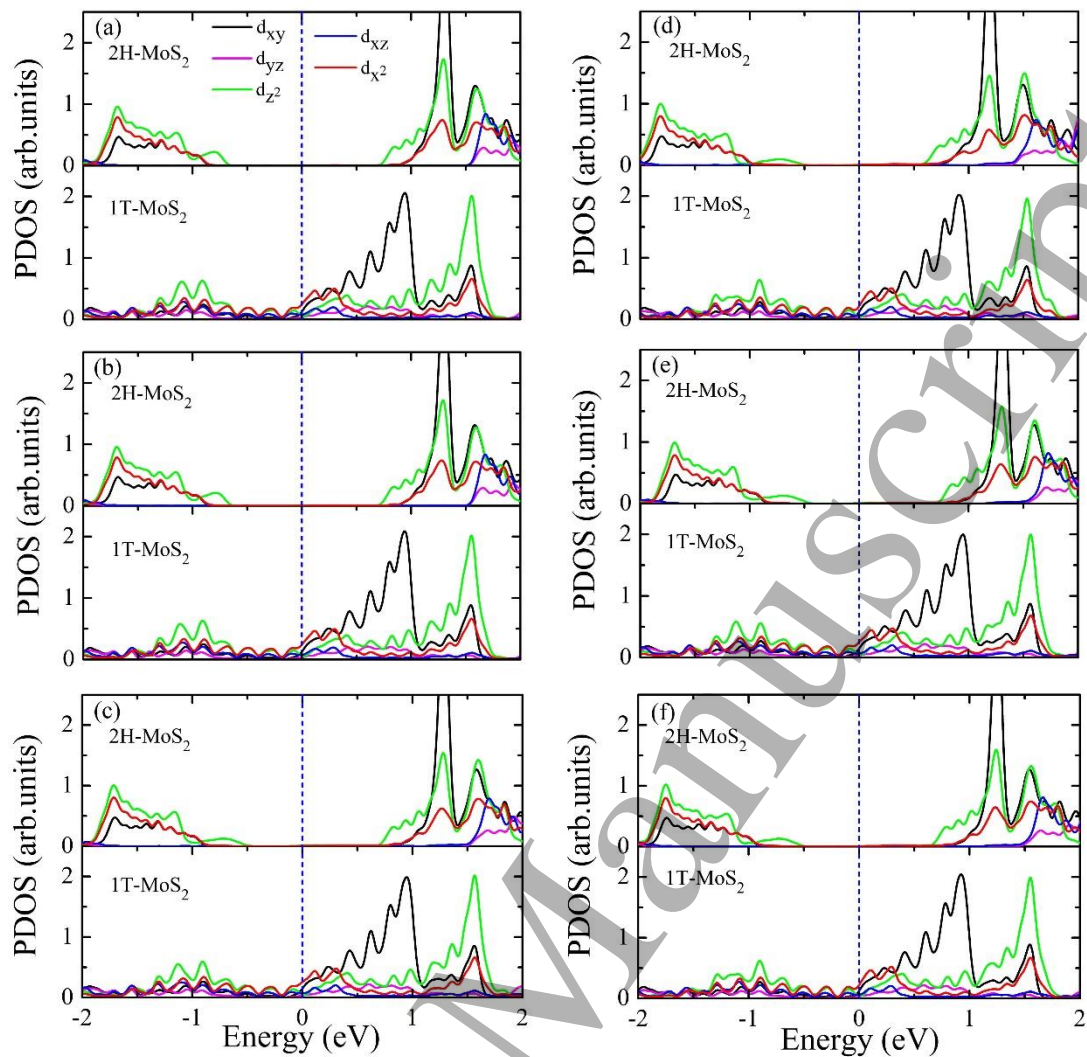


Figure 3. PDOS of 2H-MoS₂ and 1T-MoS₂ in 1T/2H MoS₂ interfaces stacked with (a) ABC, (b) ACB, (c) BAC, (d) BCA, (e) CAB, and (f) CBA, respectively. The top panel is the PDOS of 2H-MoS₂, and the bottom one is the PDOS of 1T-MoS₂. The Fermi level is indicated by the blue dashed lines.

Due to the metallic and semiconducting nature of the 1T and 2H MoS₂ monolayers, the charge transfer between the individual layers in 1T/2H MoS₂ interfaces can be expected. To examine the details of the charge transfer at the 1T/2H MoS₂ interfaces, we investigated the charge difference between the 1T/2H MoS₂

1
2
3
4 interfaces and the sum of the monolayer 2H-MoS₂ and 1T-MoS₂, i.e, $\Delta\rho = \rho_{1T/2H} - \rho_{1T}$
5
6
7 $- \rho_{2H}$ (figure S8). To have a quantitative picture, we plotted the plane-averaged
8
9 electron density difference $\Delta\rho(z)$ along the direction perpendicular to the interface
10
11 (figure 4). As shown in figure 4 (a) and (b), there is only charge depletion at the
12
13 interfacial region of ABC and ACB stacked 1T/2H MoS₂, similar to metal–graphene
14
15 contacts [44]. The presence of an interfacial charge depletion region is a direct
16
17 evidence of the surface charge repulsion effect [45]. Similar to the previous work [45],
18
19 if there is only charge depletion at the interfacial region between 1T and 2H MoS₂, the
20
21 antiparallel alignment of interface dipoles will be formed, which would reduce the
22
23 interface binding energy, as indicated by the black arrows in figure 4(g). However,
24
25 when charge accumulation also occurs at the interfacial region between 1T and 2H
26
27 MoS₂, the parallel alignment of interface dipoles will be formed, which will enhance
28
29 the interface binding energy, as shown in figure 4(h). Thus, charge accumulation at
30
31 the interfacial region could enhance the interface binding energy by tuning the
32
33 interface dipoles. In contrast, in figure 4 (c)-(f), the charge accumulation is observed
34
35 in BAC, BCA, CAB and CBA stacked 1T/2H MoS₂, which suggests a relatively
36
37 strong interaction between the two monolayers and is consistent with stronger binding
38
39 energy in BAC, BCA, CAB and CBA stacked 1T/2H MoS₂. Both the charge depletion
40
41 and the charge accumulation constitute the charge redistribution, leading to the
42
43 electric dipole formation, or the electrical polarization. Furthermore, in BAC, BCA,
44
45 CAB and CBA stacked 1T/2H MoS₂ interfaces with charge accumulation, the much
46
47 stronger charge redistribution implies more pronounced hybridization and dipole
48
49
50
51
52
53
54
55
56
57
58
59
60

formation at the interface, and consequently larger electrical polarization and striking SBH value difference between these four 1T/2H MoS₂ interfaces (0.44–0.49 eV) and those with only charge depletion at the interfacial region (namely ABC and ACB stacked 1T/2H MoS₂, 0.65–0.67 eV). The above conclusions were further substantiated by the charge difference between the 1T/2H MoS₂ interfaces and the sum of the monolayer 2H-MoS₂ and 1T-MoS₂ (figure S8).

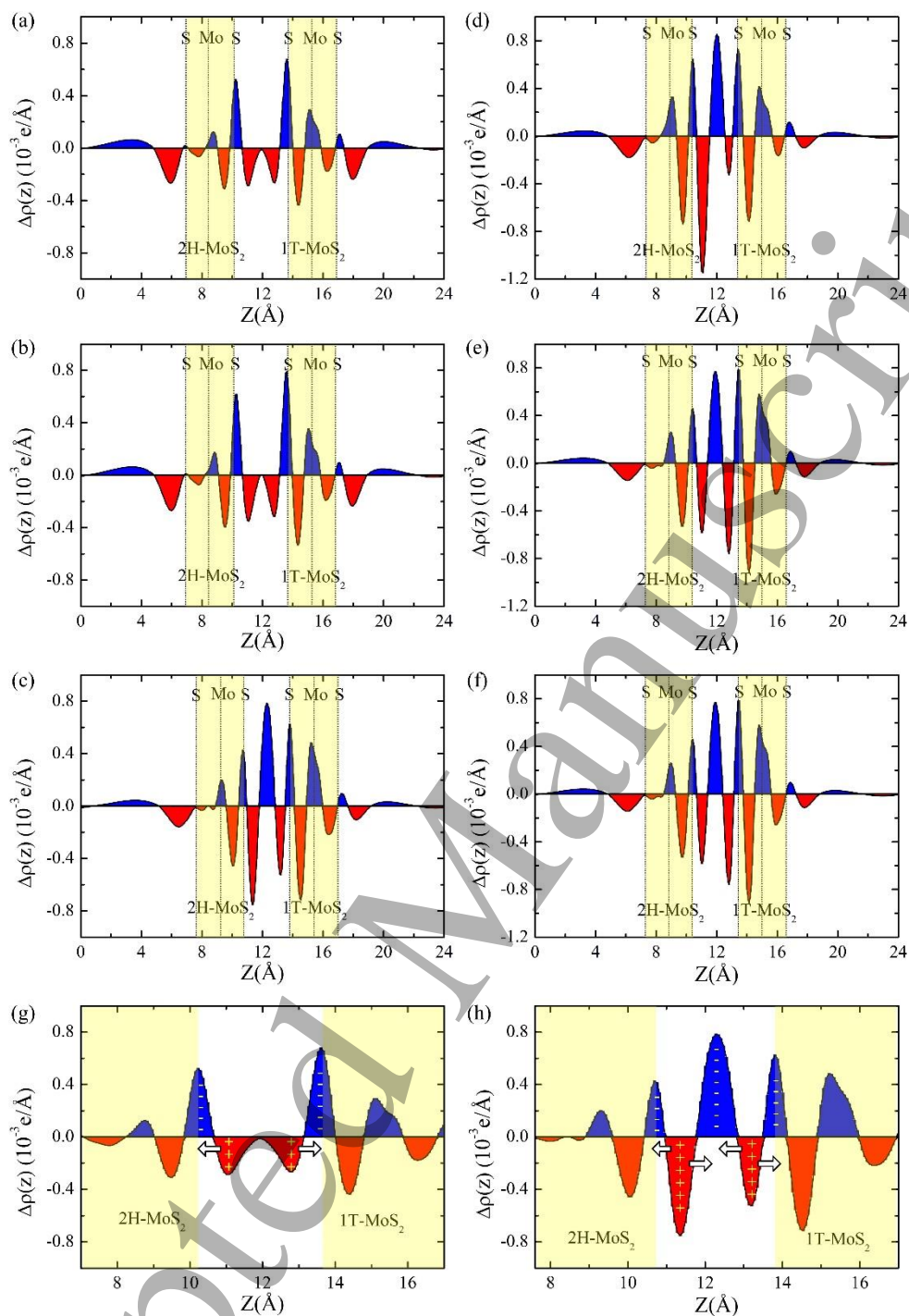


Figure 4. The plane-averaged electron density difference ($\Delta\rho(z)$) along the direction perpendicular to the interface. (a) ABC, (b) ACB, (c) BAC, (d) BCA, (e) CAB, and (f) CBA stacked 1T/2H MoS₂ interfaces. For each case, the atomic plane positions are given by the dotted lines for reference. The blue and red colors indicate electron accumulation and depletion, respectively. (g) The antiparallel alignment of interface

1
2
3
4 dipoles in ABC stacked 1T/2H MoS₂ interface, and (h) the parallel alignment of
5
6 interface dipoles in BAC stacked 1T/2H MoS₂ interface.
7
8
9

10
11 An intrinsic electric field can be introduced by the electrical polarization in the
12 1T/2H MoS₂ interfaces, and previous studies showed that the electronic structures of
13 bilayer MoS₂ can be tuned by vertical electric field [46]. Then, to what extent will the
14 electric field affect the SBH values in the 1T/2H MoS₂ interfaces? To address this
15 question, we applied an external vertical electric field across the interface, and the
16 electric field from 2H-MoS₂ to 1T-MoS₂ was defined as positive. Figure 5 presents
17 the SBH values of the 1T/2H MoS₂ interfaces under various electric fields, in which
18 the red and blue colors indicate n-type and p-type SBH values, respectively. The
19 general trend is clear: under a positive electric field, the n-type SBH consistently
20 increases with increasing electric field, while the p-type SBH generally decreases,
21 eventually achieving a significantly low p-type SBH value for all the 1T/2H MoS₂. In
22 contrast, a different response is observed when a negative electric field is applied. The
23 n-type SBH gradually decreases with increasing a negative electric field, and finally
24 achieves a significantly low n-type SBH value. In comparison, the p-type SBH
25 gradually increases under a negative electric field. Such an external
26 electric-field-dependent band alignment offers a practical route to tune the SBH
27 values.
28
29
30
31
32
33
34
35
36
37
38
39
40
41
42
43
44
45
46
47
48
49
50
51
52
53
54
55
56
57
58
59
60

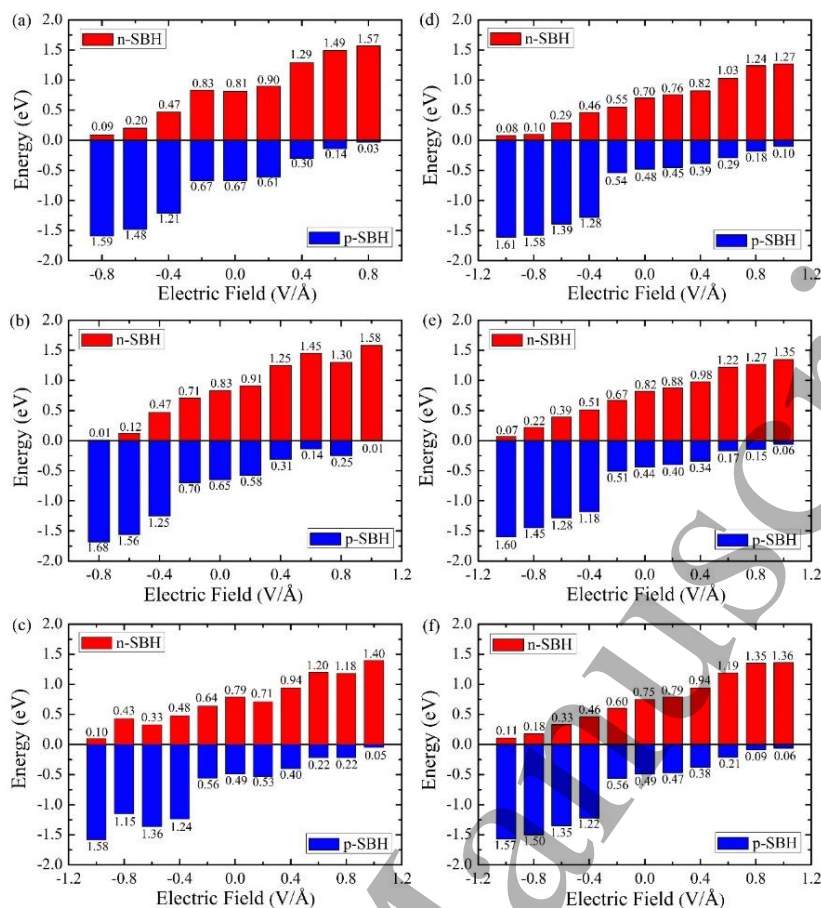


Figure 5. The electric field dependence of the n-type SBH and the p-type SBH values for (a) ABC, (b) ACB, (c) BAC, (d) BCA, (e) CAB, and (f) CBA stacked 1T/2H MoS₂ interfaces. The Fermi level is set at zero. The red and blue colors indicate n-type and p-type SBH values, respectively.

Can our above findings be extended to other 1T/2H TMDs interfaces? To address this question, we examined several other TMDs, such as WS₂, WSe₂ and MoSe₂, which have shown significant promise towards realizing p-type FETs [47–49]. Taking the BAC stacked 1T/2H TMDs interfaces as an example, we calculated their band structures, as shown in figure 6(a)-(c). The p-type SBH values (0.41, 0.66 and 0.74 eV) are lower than their corresponding n-type SBH values (0.99, 0.69 and 0.78 eV),

respectively. Furthermore, we also examined the other five stacking 1T/2H TMDs interfaces, their n-SBH and p-SBH values (table S1, Supporting Information) clearly showed that the p-type contacts are obtained in these 1T/2H interfaces. By analyzing the band alignment of monolayer 2H-WS₂, 2H-WSe₂, 2H-MoSe₂ and the work function of monolayer 1T-WS₂, 1T-WSe₂, 1T-MoSe₂ (figure 6(g)), we found that the work function of 1T-TMDs is closer to the VBM than to the CBM of 2H-TMDs, suggesting that 1T-TMDs can be used as a hole contact for 2H-TMDs. These computational results clearly demonstrate that using 1T phase as an efficient hole injection layer most likely is a universal approach to achieve p-type contacts for other TMDs (such as WS₂, WSe₂ and MoSe₂).

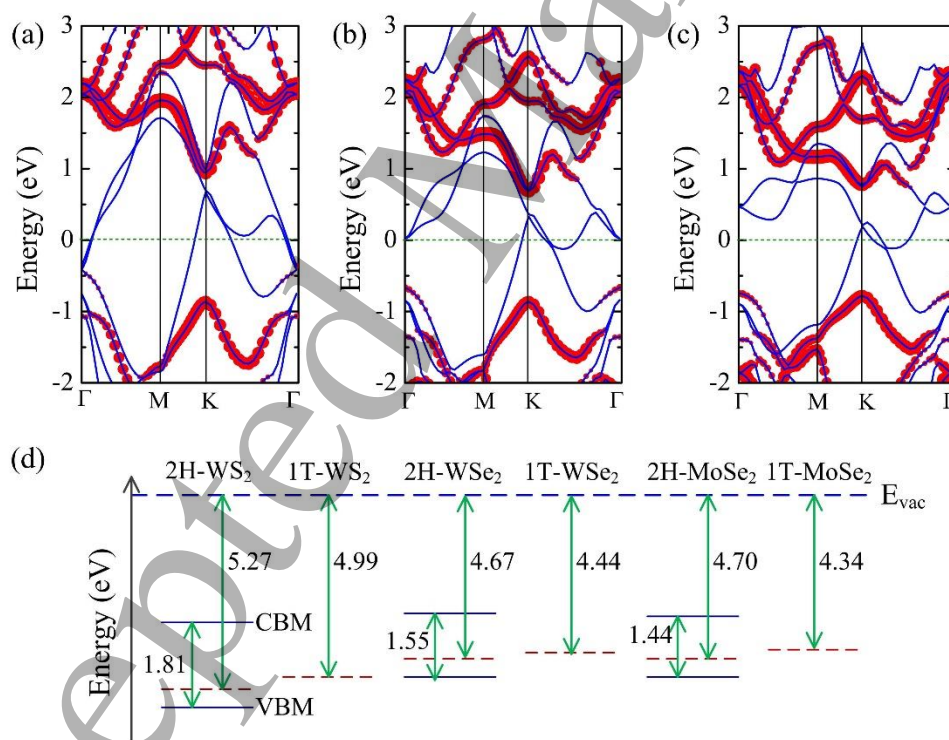


Figure 6. Band structures of 1T/2H TMDs interfaces with BAC stacking in (a) WS₂, (b) WSe₂, and (c) MoSe₂, respectively. The blue solid lines are the overall band structures. The red dots denote the projected band structures of the 2H-TMDs layer.

The weight is represented by the dot size. The Fermi level is set at zero, indicated by the olive dashed lines. (d) Band alignments of monolayer 2H-WS₂, 2H-WSe₂, 2H-MoSe₂ and the work function of monolayer 1T-WS₂, 1T-WSe₂, 1T-MoSe₂. The red dashed lines are the Fermi level. The vacuum level is taken as reference.

Conclusion

In summary, by means of comprehensive DFT calculations, we investigated carrier injection at the 1T/2H MoS₂ interface and demonstrated that the metallic 1T phase can be used as an efficient hole injection layer for 2H-MoS₂. The 1T-MoS₂ monolayer forms a p-type contact with 2H-MoS₂ due to the increase of VBM of 2H-MoS₂ upon the formation of interface and the dipole formation caused by the charge redistribution at 1T/2H MoS₂ interface. Moreover, the p-type SBH values are lower than those of the n-type Au/MoS₂ and Pd/MoS₂ contacts, which result from the efficient hole injection between 1T-MoS₂ and 2H-MoS₂. This can explain the low contact resistance in the MoS₂ FETs with 1T phase electrodes [27]. Our results also strongly support Kappera *et al*'s expectation that MoS₂ FETs with pure 1T phase electrodes will have even greater enhancement in performance than those with locally introduced 1T-MoS₂ electrodes [27]. Notably, the SBH value can be effectively modulated by an external electric field, and a significantly low p-type SBH value can be achieved under an appropriate electric field. We also demonstrated that this approach can be extended to WS₂, WSe₂, MoSe₂, and most likely other TMDs, thus it may open new promising avenues of contact engineering in TMDs.

Acknowledgements

This work is supported in China by the National Natural Science Foundation of China (Nos.11604047, 51672127), the Natural Science Foundation of Jiangsu Province (No. BK20160694), the Priority Academic Program Development of Jiangsu Higher Education Institutions (PAPD), and the open research fund of Key Laboratory of MEMS of Ministry of Education, Southeast University, and in USA by NSF-CREST Center for Innovation, Research and Education in Environmental Nanotechnology (CIRESN) (Grant Number HRD-1736093). AVK acknowledges the Academy of Finland for the support under Project No. 286279. We also thank CSC Finland for generous grants of computer time.

References

- [1] Wang Q H, Kalantar-Zadeh K, Kis A, Coleman J N, Strano M S 2012 Electronics and optoelectronics of two-dimensional transition metal dichalcogenides *Nat. Nanotechnol.* **7** 699–712
- [2] Allain A, Kang J, Banerjee K, Kis A 2015 Electrical contacts to two-dimensional semiconductors *Nat. Mater.* **14** 1195–1205
- [3] Duan X, Wang C, Pan A, Yu R, Duan X 2015 Two-dimensional transition metal dichalcogenides as atomically thin semiconductors: opportunities and challenges *Chem. Soc. Rev.* **44** 8859–8876
- [4] Lembke D, Bertolazzi S, Kis A 2015 Single-layer MoS₂ electronics *Acc. Chem. Res.* **48** 100–110
- [5] Chhowalla M, Jena D, Zhang H 2016 Two-dimensional semiconductors for

- transistors *Nat. Rev. Mater.* **1** 16052
- [6] Manzeli S, Ovchinnikov D, Pasquier D, Yazyev O V, Kis A 2017 2D transition metal dichalcogenides *Nat. Rev. Mater.* **2** 17033
- [7] Ma Y, Kou L, Li X, Dai Y, Heine T 2016 Two-dimensional transition metal dichalcogenides with a hexagonal lattice: room-temperature quantum spin Hall insulators. *Phys. Rev. B* **93** 035442
- [8] Kou L, Frauenheim T, Chen C 2013 Nanoscale multilayer transition-metal dichalcogenides heterostructures: band gap modulation by interfacial strain and spontaneous polarization *J. Phys. Chem. Lett.* **4** 1730–1736
- [9] Chuang S et al 2014 MoS₂ p-type transistors and diodes enabled by high work function MoO_x Contacts *Nano Lett.* **14** 1337–1342
- [10] Liu H, Neal A T, Ye P D 2012 Channel length scaling of MoS₂ MOSFETs *ACS Nano* **6** 8563–8569
- [11] Qiu H, Pan L, Yao Z, Li J, Shi Y, Wang X 2012 Electrical characterization of back-gated bi-layer MoS₂ field-effect transistors and the effect of ambient on their performances *Appl. Phys. Lett.* **100** 123104
- [12] Kim S et al 2012 High-mobility and low-power thin-film transistors based on multilayer MoS₂ crystals *Nat. Commun.* **3** 1011
- [13] Lemme M C, Li L, Palacios T, Schwierz F 2014 Two-dimensional materials for electronic applications *MRS Bulletin* **39** 711–718
- [14] Fontana M, Deppe T, Boyd A K, Rinzan M, Liu A Y, Paranjape M, Barbara P 2013 Electron-hole transport and photovoltaic effect in gated MoS₂ schottky

- junctions *Sci. Rep.* **3** 1634
- [15] McDonnell S, Azcatl A, Addou R, Gong C, Battaglia C, Chuang S, Cho K, Javey A, Wallace R M 2014 Hole contacts on transition metal dichalcogenides: interface chemistry and band alignments *ACS Nano* **8** 6265–6272
- [16] Mak K F, Lee C, Hone J, Shan J, Heinz T F 2010 Atomically thin MoS₂: a new direct-gap semiconductor *Phys. Rev. Lett.* **105** 136805
- [17] Radisavljevic B, Radenovic A, Brivio J, Giacometti V, Kis A 2011 Single-layer MoS₂ transistors *Nat. Nanotechnol.* **6** 147–150
- [18] Gong C, Colombo L, Wallace R M, Cho K 2014 The unusual mechanism of partial fermi level pinning at metal-MoS₂ interfaces *Nano Lett.* **14** 1714–1720
- [19] Chen W, Santos E J G, Zhu W G, Kaxiras E, Zhang Z Y 2013 Tuning the electronic and chemical properties of monolayer MoS₂ adsorbed on transition metal substrates *Nano Lett* **13** 509–514
- [20] Zhong H et al 2016 Interfacial properties of monolayer and bilayer MoS₂ contacts with metals: beyond the energy band calculations. *Sci. Rep.* **6** 21786
- [21] Musso T, Kumar P V, Foster A S, Grossman J C 2014 Graphene oxide as a promising hole injection layer for MoS₂-based electronic devices *ACS Nano* **8** 11432–11439
- [22] Eda G, Chhowalla M 2010 Chemically derived graphene oxide: towards large-area thin-film electronics and optoelectronics *Adv. Mater.* **22** 2392–2415
- [23] Voiry D, Mohite A, Chhowalla M 2015 Phase engineering of transition metal dichalcogenides *Chem. Soc. Rev.* **44** 2702–2712

- [24] Lin Y, Dumcenco D O, Huang Y, Suenaga K 2014 Atomic mechanism of the semiconducting-to-metallic phase transition in single-layered MoS₂ *Nat. Nanotechnol.* **9** 391–396
- [25] Kretschmer S, Komsa H, Boggild P, Krashenninnikov A V 2017 Structural transformations in two-dimensional transition-metal dichalcogenide MoS₂ under an electron beam: insights from first-principles calculations *J. Phys. Chem. Lett.* **8** 3061–3067
- [26] Kim J S et al 2016 Electrical transport properties of polymorphic MoS₂ *ACS Nano* **10** 7500–7506
- [27] Kappera R, Voiry D, Yalcin S E, Branch B, Gupta G, Mohite A D, Chhowalla M 2014 Phase-engineered low-resistance contacts for ultrathin MoS₂ transistors *Nat. Mater.* **13** 1128–1134
- [28] Chhowalla M, Shin H S, Eda G, Li L J, Loh K P, Zhang H 2013 The chemistry of two-dimensional layered transition metal dichalcogenide nanosheets *Nat. Chem.* **5** 263–275
- [29] Eda G, Fujita T, Yamaguchi H, Voiry D, Chen M W, Chhowalla M 2012 Coherent atomic and electronic heterostructures of single-layer MoS₂ *ACS Nano* **6** 7311–7317
- [30] Lukowski M A, Daniel A S, Meng F, Forticaux A, Li L, Jin S 2013 Enhanced hydrogen evolution catalysis from chemically exfoliated metallic MoS₂ nanosheets *J. Am. Chem. Soc.* **135** 10274–10277
- [31] Wang L, Liu X, Luo J, Duan X, Crittenden J, Liu C, Zhang S, Pei Y, Zeng Y,

- Duan X 2017 Self-optimization of the active site of molybdenum disulfide by an irreversible phase transition during photocatalytic hydrogen evolution *Angew. Chem. Int. Ed.* **56** 7610-7614
- [32] Kappera R et al 2014 Metallic 1T phase source/drain electrodes for field effect transistors from chemical vapor deposited MoS₂ *APL Mater.* **2** 092516
- [33] Kresse G, Furthmüller J 1996 Efficient iterative schemes for ab initio total-energy calculations using a plane-wave basis set *Phys. Rev. B* **54** 11169–11186
- [34] Kresse G, Furthmüller J 1996 Efficiency of ab initio total energy calculations for metals and semiconductors using a plane-wave basis set *Comput. Mater. Sci.* **6** 15–50
- [35] Blöchl P E 1994 Projector augmented-wave method *Phys. Rev. B* **50** 17953–17979
- [36] Kresse G, Joubert D 1999 From ultrasoft pseudopotentials to the projector augmented-wave method *Phys. Rev. B* **59** 1758–1775
- [37] Perdew J P, Burke K, Ernzerhof M 1996 Generalized gradient approximation made simple *Phys. Rev. Lett.* **77** 3865–3868
- [38] Grimme S 2006 Semiempirical GGA-type density functional constructed with a long-range dispersion correction *J. Comput. Chem.* **27** 1787–1799
- [39] Bučko T, Hafner J, Lebègue S, Ángyán J G 2010 Improved description of the structure of molecular and layered crystals: ab-initio DFT calculations with van der Waals corrections *J. Phys. Chem. A* **114** 11814–11824

- [40] Gao G, Jiao Y, Ma F, Jiao Y, Waclawik E, Du A 2015 Charge mediated semiconducting-to-metallic phase transition in molybdenum disulfide monolayer and hydrogen evolution reaction in new 1T' Phase *J. Phys. Chem. C* **119** 13124–13128
- [41] Kan M, Wang J Y, Li X W, Zhang S H, Li Y W, Kawazoe Y, Sun Q, Jena P 2014 Structures and phase transition of a MoS₂ monolayer *J. Phys. Chem. C* **118** 1515–1522
- [42] Liu Y et al 2015 Toward barrier free contact to molybdenum disulfide using graphene electrodes *Nano Lett.* **15** 3030–3034
- [43] Padilha J E, Peelaers H, Janotti A, Van de Walle C G 2014 Nature and evolution of the band-edge states in MoS₂: from monolayer to bulk *Phys. Rev. B* **90** 205420
- [44] Gong C, Lee G, Shan B, Vogel E M, Wallace R M, Cho K 2010 First-principles study of metal-graphene interfaces *J. Appl. Phys.* **108** 123711
- [45] Gong C, Hinojos D, Wang W, Nijem N, Shan B, Wallace R M, Cho K, Chabal Y J 2012 Metal–graphene–metal sandwich contacts for enhanced interface bonding and work function control *ACS Nano* **6** 5381–5387
- [46] Liu Q, Li L, Li Y, Gao Z, Chen Z, Lu J 2012 Tuning electronic structure of bilayer MoS₂ by vertical electric field: a first-principles investigation *J. Phys. Chem. C* **116** 21556–21562
- [47] Fang H, Chuang S, Chang T C, Takei K, Takahashi T, Javey A 2012 High-performance single layered WSe₂ p-FETs with chemically doped contacts *Nano Lett.* **12** 3788

- [48] Chuang H, Chamlagain B, Koehler M, Perera M M, Yan J, Mandrus D, Tomnek D, Zhou Z 2016 Low-resistance 2D/2D ohmic contacts: a universal approach to high-performance WSe₂, MoS₂, and MoSe₂ transistors *Nano Lett.* **16** 1896
- [49] Huang L, Zhong M, Wei Z, Li J 2017 Tunable schottky barrier at MoSe₂/metal interfaces with a buffer layer *J. Phys. Chem. C* **121** 9305–9311